

Full Paper

Heidi Fearn^{1*}, James F. Woodward²

Experimental null test of a Mach effect thruster

¹Department of Physics, California State University, Fullerton, CA, 92834, (UNITED STATES)

²Department of Physics, Senior Member AIAA, California State University, Fullerton, CA, 92834, (UNITED STATES)

E-mail: hfearn@fullerton.edu; jwoodward@fullerton.edu

Received: April 15, 2013

Accepted: June 01, 2013

Published: July 29, 2013

Abstract

The Mach Effect Thruster (MET) is a device which utilizes fluctuations in the rest masses of accelerating objects (lead-zirconium-titanate, PZT stacks, in which internal energy changes take place) to produce a steady linear thrust. The theory has been given in detail elsewhere^[1,2] and references therein, so here we discuss only an experiment. We show the stack of PZT disks being used as a thruster and then eliminate the thrust by arranging equal brass masses on either end, so that essentially the PZT stack is trying to push in both directions at once. This arrangement in theory would only allow for a small oscillation but no net thrust. We find the thrust does indeed disappear in the experiment, as predicted. The device (in thruster mode) could in principle be used for propulsion^[1,2]. Experimental apparatus based on a very sensitive thrust balance is briefly described. The experimental protocol employed to search for expected Mach effects is laid out, and the results of this experimental investigation are described.

*Corresponding author's Name & Add.

Keywords

Mach effect thruster; Exotic propulsion; Propellantless engine; Gravitational inertia.

Heidi Fearn
Department of Physics, California State University, Fullerton, CA, 92834, (UNITED STATES)
E-mail: hfearn@fullerton.edu

INTRODUCTION

Mach effects are the fluctuations in the rest masses of extended objects when they are accelerated by external forces and at the same time undergo deformations during acceleration. The deformations correspond to internal energy changes of the accelerated mass. These proper mass fluctuations are not simply due to changes in E/c^2 in an accelerating object. They arise through the gravitational coupling of the accelerating mass to the rest of the matter in the universe. In fact the Mach effect changes in proper mass are much larger than the E/c^2 changes due to energy stored in the accelerating object, say a capacitor. The theory of the Mach effect thruster (MET) has been addressed in detail elsewhere^[1,2] so here we only give a brief overview of the main results and calculate values pertaining to this particular experiment. When we identify inertial mass as being due to gravitational interactions with the rest of the mass and energy flow in the universe, we open up the possibility of mass fluctuations. For the Mach effect proper

mass fluctuation δm_0 we get^[1,2],

$$\delta m_0 = \frac{1}{4\pi G} \left[\frac{1}{\rho_0 c^2} \frac{\partial P}{\partial t} - \left(\frac{1}{\rho_0 c^2} \right)^2 \frac{P^2}{V} \right] \quad (1)$$

V in this equation is the volume of the object to which the power P is applied. Where G is the gravitational constant, c is the velocity of light in a vacuum, and ρ_0 is the rest mass density of the accelerating object. If we ignore the smaller second term in Eq. (1) we may write the proper mass fluctuation as,

$$\delta m_0 \approx \frac{1}{4\pi G} \left[\frac{1}{\rho_0 c^2} \frac{\partial P}{\partial t} \right] \approx \frac{1}{4\pi G \rho_0 c^2} \mathbf{F} \bullet \mathbf{a} \quad (2)$$

since $P = dE/dt = d/dt(F \cdot dx) = F \cdot v$ and $dP/dt = F \cdot a$. Note that the mass fluctuation predicted here only occurs in an object that is being accelerated as the power fluctuates. If no "bulk" acceleration of the object takes place, there is no Mach type mass fluctuation.

Noting that $F=ma$, the mass fluctuation can be written as,

$$\delta m_0 \approx \frac{1}{4\pi G \rho_0 c^2} m_0 a^2 \quad (3)$$

Evidently, *the simplest* Mach effect depends on the square of the acceleration of the body in which it is produced.

THE MACH EFFECT DEVICE

The devices tested consisted of stacks of 19mm diameter by 1 mm thick lead-zirconium-titanate (PZT) crystals glued together with brass electrodes, see Figure 1. The stack (labeled N4) had sixteen crystals. Polarized, they are arranged plus to plus and minus to minus with brass electrodes (0.051mm thickness) interspersed between them. The stack also had 3 embedded accelerometers, made with two 0.3 mm thick crystals each, making the PZT stack length 19 mm. The accelerometers were located at both ends and one 1/4 of the way through the PZT stack. The crystals are Steiner-Martins mixture SM-111. For thruster mode testing, the PZT stacks were clamped between a thin (4 mm thick) aluminum end cap and a thicker (12.7 mm thick) brass disk. The disk acted as a reaction mass against which the mechanical action of the stack took place. The 4-40 screws were torqued between 8-9 inch pounds.

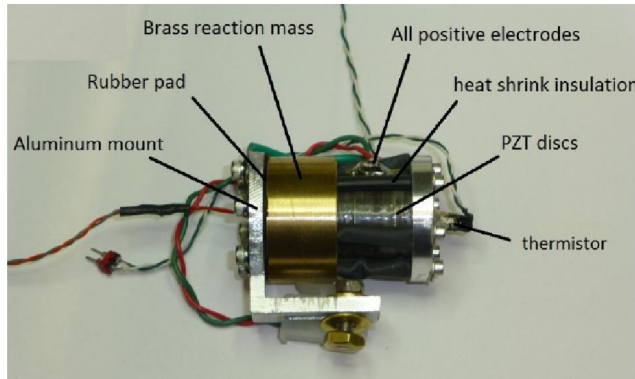


Figure 1 : The Mach effect device is a stack of PZT discs, which are capacitors. Sixteen 1 mm PZT discs were glued together to form the stack. These are then bolted to a reaction mass using 4-40 insulated bolts. The electrodes are made from 0.002inch brass sheet. There are 3 accelerometers present, at the front and back of the stack and one 1/4 way through.

Additional theory for Mach effect force

The stack of PZT crystals is shown capable of producing a static thrust. The production of thrust depends on combining periodic mass fluctuations with a periodic force at the frequency of the fluctuations. The phase of the force and the mass fluctuation needs to be the same to deliver maximum thrust.

Since the chief response of the PZT stack is piezoelectric (that is, linear in the voltage), the chief displacement, ve-

locity, and acceleration induced will occur at the frequency of the applied signal. The square of the acceleration will produce a mass fluctuation with twice the frequency of the applied voltage signal. In order to transform the mass fluctuation into a stationary force, a second (electro) mechanical force must be supplied at twice the frequency of the force that produces the mass fluctuation. In these crystals there is no need to apply a second force since electrostriction is already present. The electrostriction is dependent on V^2 and thus has the correct frequency and phase dependence.

Calculation of the interaction of the electrostrictive electromechanical effect with the predicted mass fluctuation is straight-forward. We apply a periodic voltage to the PZT stack,

$$V = V_0 \cos \omega t \quad (4)$$

Including the piezoelectric displacement and the electrostrictive displacement, the length of the PZT stack is approximately:

$$x = x_0(1 + K_p V + K_e V^2) = x_0(1 + K_p V_0 \cos \omega t + K_e V_0^2 \cos^2 t) \quad (5)$$

where x_0 the length for zero voltage and K_p and K_e are the piezoelectric and electrostrictive constants of the material respectively. Eq. (5) is valid for off resonant frequencies and in general one must integrate the longitudinal strain over the length of the PZT stack to obtain the net increase in length and thus the acceleration. We use Eq. (5) as an approximation only, the actual length increase near resonance is larger due to resonance amplification. The frequencies used are between 30-45 KHz. They are at the very low end of the PZT resonances. See for example, the finite element modeling by Jan Kobach^[3]. The velocity and acceleration are just the first and second time-derivatives (respectively) of Eq. (5). The acceleration and the mass fluctuation are,

$$a = \ddot{x} = -\omega^2 x_0 (K_p V_0 \cos \omega t + K_e V_0^2 \cos 2\omega t) \quad (6)$$

The mass change becomes

$$\delta m_0 = \frac{m_0 \omega^4 x_0^2}{8\pi G \rho_0 c^2} \left[K_p^2 V_0^2 (1 + \cos 2\omega t) + K_e^2 V_0^4 (1 + \cos 4\omega t) + 4K_p K_e V_0^3 \cos \omega t \cos 2\omega t \right] \quad (7)$$

The largest term in Eq.(7) is the one which goes as $K_p^2 V_0^2$ since the electrostrictive constant is much smaller than the piezoelectric constant. Treating the electrostrictive part of the motion separately, electrostriction produces a displacement proportional to the square of the applied voltage,

$$x = x_0(1 + K_e V^2) = x_0(1 + K_e V_0^2 \cos^2 \omega t) \quad (8)$$

The acceleration due to electrostriction becomes,

$$\alpha = -2\omega^2 K_e x_0 V_0^2 \cos 2\omega t \quad (9)$$

Terms which produce a DC or stationary force involve

the product of the piezoelectric coefficient squared and the electrostrictive coefficient. The magnitude of the force is approximately,

$$|F| = \delta m_0 a = \frac{m_0 \omega^6 K_p^2 K_e^2 x_0^3 V_0^4}{8\pi G \rho_0 c^2} \left[K_p^2 + K_p^2 (2 \cos 2\omega t + \cos 4\omega t) + 2K_e^2 V_0^2 \cos 2\omega t (1 + \cos 4\omega t) + 4K_p K_e V_0 \cos \omega t (1 + \cos 4\omega t) \right] \quad (10)$$

All the trigonometric terms time-average to zero and the resulting time-average $|F|$ is

$$\langle F \rangle \approx \frac{\omega^6 m_0 K_p^2 K_e^2 x_0^3 V_0^4}{8\pi G \rho_0 c^2} \quad (11)$$

To get a sense for the type of thrusts predicted by the Mach effect, we substitute values for a PZT stack device used in the experimental work reported here into Eq. (11). The resonant frequencies for this device is 32.35 KHz (in thrust mode) and 42 KHz (in null mode). The frequency 32.35 KHz is used as a nominal resonant frequency. Expressing this as an angular frequency and raising it to the sixth power, we get 7.05×10^{31} . The rest mass of the PZT stack is 46 g and the whole stack is active. The length of the stack is 19 mm. In most circumstances the voltage at resonance is about 100 volts at an average power level. And the density of SM-111 material is 7.9 g/cc, or $\rho_0 = 7.9 \times 10^3 \text{ kgm}^{-3}$ ^[4]. We use the SI values of $G = 6.672 \times 10^{-11} \text{ m}^3 \text{ s}^{-2} \text{ kg}^{-1}$ and $c = 2.9979 \times 10^8 \text{ ms}^{-1}$, and set aside the values of the piezoelectric and electrostrictive constants for the moment. Inserting all of these values, converting from Gaussian units to S.I. using 4π gives,

$$\langle F \rangle \approx 2.35 \times 10^{-22} K_p^2 K_e^2 \quad (12)$$

Steiner-Martins give $3.2 \times 10^{-10} \text{ mV}^{-1}$ for the “ d_{33} ” piezoelectric constant for the SM-111 material^[4]. That is the value of K_p . Using the value for K_p we find

$$\langle F \rangle \approx 2406.3 K_e^2 \quad (13)$$

Steiner-Martins list no value for the electrostrictive constant. But electrostrictive effects are generally smaller than piezoelectric effects^[5-7]. From the power spectrum of the voltage across the capacitor stack, it is possible to estimate that the electrostrictive constant must be somewhere between $1/6^{\text{th}}$ and $1/10^{\text{th}}$ of the piezoelectric constant. The resonant frequency vs. power was plotted on an oscilloscope^[1] and the scale shows that the second harmonic frequency power was approximately $1/8^{\text{th}}$ of the power of the first harmonic. (There was a few dB drop in power for the second harmonic.) The electrostrictive constant taken is consistent with the references^[5-7]. Taking the electrostrictive constant to be $1/8^{\text{th}}$ of the piezoelectric constant, or approximately $4 \times 10^{-11} \text{ mV}^{-2}$, the thrust is found to be 96 nN. No allowance for mechanical resonance amplification is made. Inspection of the plots sug-

gests that this effect may contribute significantly to the observed effects, lifting the thrust into the micro Newton range.

THRUST EXPERIMENT SETUP AND RESULTS

To test for the presence of proper matter density fluctuations of the sort predicted in Eqs. (3) and (7) we subject a stack of PZT disk capacitors to large, rapid voltage fluctuations. Capacitors store energy in the electric field between the plates or, as in this case, in the electric polarization of the dielectric medium by ion core displacements. The condition that the capacitor restmass vary in time is met as the ions in the lattice are accelerated by the changing external electric field. If the amplitude of the proper energy density variation and its first and second time derivatives are large enough, a small (10^{-11} Kg) mass fluctuation should ensue. That mass fluctuation, δm_0 , is given by Eqn. (8) above. *Note that the assumption that all of the power delivered to the capacitors ends up as a proper energy density fluctuation is an optimistic assumption. Some of this energy is likely stored in the gravitational field, and some will dissipate as heat.* Nonetheless, it is arguably a reasonable place to start.

Note too that simply charging and discharging capacitors will produce mass fluctuations of the $m = E/c^2$ variety, but these are very small and do not lead to any detectable effect. The electromagnetic text books now refer to “hidden momentum”, which is simply the flow of energy from one part of an isolated circuit to another, introducing a center of mass shift and therefore a shift in position of the capacitor relative to the power source. This is very tiny, of the order $\delta m = CV^2/(2c^2) = 1.1 \times 10^{-17} \text{ Kg}$ which corresponds to 200 μF capacitor charged to 100 Volts, or the mass change for 1 Joule of energy stored. This will not lead to any net effect only oscillation as the capacitor is charged and discharged.

A single disk of PZT has a capacitance of approximately 3.51 nF. This varies slightly from disk to disk. The PZT stack, of 16 discs, is connected in parallel, hence its ideal capacitance would be 56nF. The measured capacitance of the entire PZT stack is 36.8 nF, so that the effective energy-mass fluctuation is $2.04 \times 10^{-21} \text{ Kg}$ for 100 Volts, much smaller than the Mach effect mass fluctuation. In fact the ratio of Mach mass change to E/c^2 mass change is of the order 10^{10} or approximately $(1/4\pi G)$. Only the Mach effect mass fluctuation is considered for our PZT capacitor stack.

Experimental setup

While energy is being stored in a PZT stack, a mechanical acceleration of the device is produced by the linear (in voltage) piezoelectric effect and the quadratic (in volt-

age) electrostrictive effect. One of these devices mounted on an aluminum bracket in its Faraday cage on the end of a thrust balance beam is shown in Figure 2(a). The Faraday cage is an aluminum project box lined with mu-metal, with the top removed so that the enclosed device can be seen.

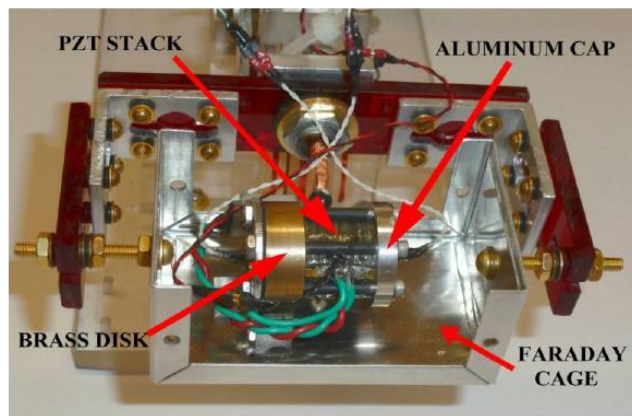


Figure 2(a) : A PZT stack device mounted in a Faraday cage on the beam of a thrust balance.

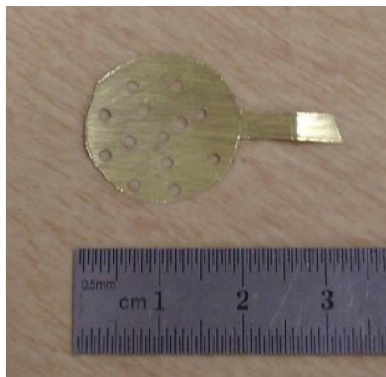


Figure 2(b) : Electrodes are hand cut from 0.002inch thick brass sheet ($5.05 \times 10^{-5}\text{m}$). A stack of brass sheets are clamped and drilled with holes. This helps with adhesion. They are then cut to size and sanded. The glue used is a 50:50 mixture of Versamid 140 and shell Epon Resin 815C. All the positive contacts line up and all the ground contacts line up, and all the accelerometer positives line up separately and are separately soldered together. You can see the soldered power contacts in Figure 1.

Note that the mounting bracket is an “L” shape aluminum bracket attached at the brass end of this device. There is a brass screw, with plastic washers, at the bottom of the device to attach to the Faraday cage.

The thrust produced by the device, shown in Figure 1, was detected using a thrust balance designed, with modest signal averaging, to be able to detect thrusts on the order of tenths of microNewtons. The thrust balance was based on a pair of C-Flex flexural bearings. Of special note are the three liquid metal contacts located coaxially above the support bearings used to transfer power to the device on the end of the beam.

This is to avoid large current carrying wires (with associ-

ated magnetic fields) near the calibration coils. Calibration of the balance is achieved using three 10 turn coils. The two outer coils are affixed to the balance platform; and the third coil is located midway between the outer coils and attached to the balance beam. The coils are wired in series, with the poles reversed, and a current through them produces a known force on the beam. The displacement by the force is measured with the optical position sensor located at the other end of the beam. The motion of the beam is damped by a pair of aluminum plates attached to the beam that move in the magnetic field of an array of small neodymium-boron magnets. The power circuit was extensively shielded to insure that stray fields did not contaminate the results.

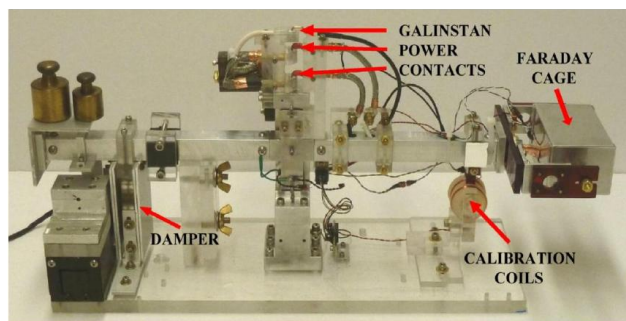


Figure 3 : The thrust balance used in the experiment whose results are reported here. C-flex flexural bearing in the central column support the balance beam and provide the restoring torque for thrust measurements. The position of the beam is sensed with a Philtec D63 optical position sensor whose probe is attached to the stepper motor to the left of the damper.

The electronics for this experiment fall into three general categories: the power circuit, the instrumentation circuits, and the computer control and data acquisition system. The last of these was based on a Canetics analog to digital converter board (8 AD channels with 12 bit resolution) supplemented by to digital to analog (DA) channels. One of the DA channels was used to switch the power signal to the power amplifier. The other was used to modulate the frequency of the signal generator so that sweeps of selected frequency ranges could be carried out in the data acquisition process. The AD channels recorded the output of the thrust sensor, the (rectified) amplitude of the voltage across the device, the amplitude of the (rectified) voltage signal generated by the accelerometer embedded in the active part of the PZT stack, and the temperature of the aluminum cap (in immediate proximity to the active part of the PZT stack). Other temperature and accelerometer measurements were made at various times. But for the results reported here, only the aforementioned data channels are relevant.

The power circuit consisted of two parts: the power amplifier, and the signal generator that produced the amplified signal. The signal generator was based on the Elenco

Function Blox signal generator board. This board, in addition to allowing the selection of frequency range and signal waveform, provides for both amplitude and frequency modulation. For this experiment, only the sine waveform was used, and the frequency range was 10 to 100 KHz. The Mach effect sought depends on operation at the resonant frequency of the device. Frequency modulation was used to scan a range of frequencies so that resonant frequencies could be identified. Our signal generator is a voltage controlled oscillator, so by sweeping a small range of low voltages it is possible to control the frequency of the swept signal. The power amplifier employed was a Carvin DCM 1000 operating in bridged mode. All of the instrumentation channels were provided with unity gain buffers and instrumentation amplifiers (to protect other circuitry and insure that the signal recorded was referenced to local ground) and provided with (50 Hz low pass) anti-aliasing filters. The thrust sensor was also provided with an offset and high gain amplifier (to resolve small signals riding on a ~ 5 volt signal), as these available options had not been purchased with the original Philtech device. Oscilloscopes and meters were employed for real-time monitoring of the AC and DC signals.

Calibration of thrust balance

The force from the double coils can easily be calculated from the mutual inductance of two coaxial coils by Babic and Akyel^[8] using elliptic functions. Eq. (3) in reference^[8] gives the force between 2 coils (so this is double) as,

$$F = \frac{\mu_0 n^2 i^2 k z}{2r} \left[\frac{(2-k^2)}{(1-k^2)} E(k) - 2K(k) \right] \quad (14)$$

where

$$k^2 = \frac{4r^2}{4r^2 + z^2}$$

The coil radius is r (1.75cm), the separation is z (1cm) so $k = 0.96$ ($k = \sin \psi$ gives $\psi = 74^\circ$) and the elliptic functions (of the first and second kind) become $K(74^\circ) = 2.708$ and $E(74^\circ) = 1.084$ from tables. The number of turns on each coil is $n = 10$, so the calibration coils provide a force,

$$F = 326.7 \times 10^{-6} i^2 \quad (15)$$

where i is the current through the coils. A coil current of 500mA gives a force of 82μN. See Figure 3 for the calibration coil setup.

The data for the C-Flex bearings in the center column of the thrust balance can be found in reference^[9]. The radial stiffness of the E-10 bearing is quoted as 1.4×10^{-4} inches deflection per pound of load.

The conversion of 1 lb = 0.453 kg and 1 inch = 2.54 cm. We convert the torque to S.I. units as follows,

$$1 \text{ lb in} = 0.453 \times 9.81 \times 2.54 \times 10^{-2} \text{ Nm} = 0.1129 \text{ Nm.}$$

So a torque $\tau = 1.4 \times 10^{-4}$ lb in converts to 11.3×10^{-6}

Nm. There are two C-Flex bearing in our thrust balance so the torque will be $\tau = 22.6 \times 10^{-6}$ Nm.

The Philtec D63 optical sensor manual gives the ideal sensitivity of the probe $\alpha = 2.441 \text{ mV}/\mu\text{Inch} = 96.1 \times 10^3 \text{ V/m}$, where $V = \alpha x$, and x is the displacement measured by the sensor. A sensor voltage of 450mV gives a displacement of 4.68μm. Let us take $F = \beta x$, then using a force (from the coils) of 3.2μN (from 100mA through the coils) shows an accelerometer voltage 450mV which in turn gives $\beta = 683.76 \times 10^{-3} \text{ N/m}$ or $F = (\beta/\alpha)V = 7.1 \times 10^{-6} \text{ V}$. This will be a slight over estimate since we took ideal sensitivity. From actual measurements of thrust sensor voltage verse force (from the coils) a least squares fit to the data (see TABLE 1.) gives,

$$F(V) = -0.0145 + 6.1 \times 10^{-3} V \quad (16)$$

where the voltage here is in mV and the force is in μN. This agrees quite well with our theoretical prediction.

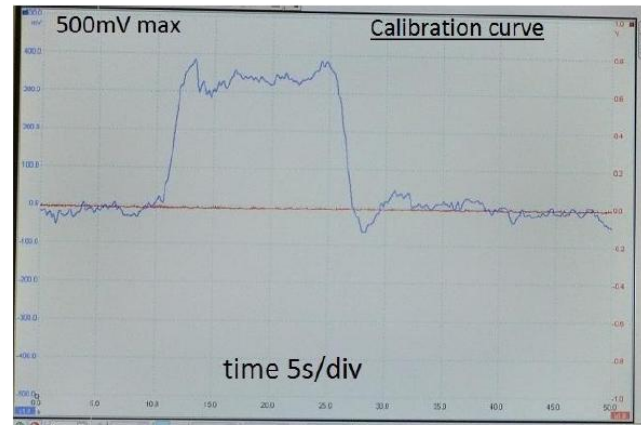


Figure 4 : The response of the balance to a calibration force. The force is applied for 15 seconds. Note there is minimal overshoot upon relaxation since the beam is nearly critically damped. The force vs. voltage calibration gives $F(V) = -0.01448 + 0.006139V$, (for force in microNewtons and voltages in milivolts) or 200mV gives 1.23 μN.

TABLE 1

Applied Coil Current (mA)	Thrust Sensor Voltage (mV)	Force from Coils (μN)
32	100	0.33
50	150	0.80
100	450	3.20
200	2100	12.80

Experimental procedure

The device was setup as in Figure 2(a). Depending on the experiment in progress, either one or two brass masses were attached to the PZT stack and then the entire device inserted in the Faraday cage mounted on the end of the thrust balance. Using an approximately 100 Volts applied amplitude signal, we found a resonance at frequency 32.35 KHz. This was chosen as the “center” frequency for the sweeps. Each “run” consisted of taking data for 32 sec-

onds. The first 8 seconds were quiescent data to establish the background noise. This was followed by a 1 second power pulse at the center frequency. Then the sweep through 10 KHz over 8 seconds commenced. After the sweep was completed, another 1 second power pulse at the center frequency was applied. The remainder of the 32 seconds was quiescent data.

Signal averaging was done by taking typically a dozen runs in exactly the same circumstances and averaging them to suppress random noise. In order to suppress spurious signals, runs were done with the device facing “forward” on the end of the balance, and also “reversed”, that is, with the device and Faraday cage rotated 180 degrees on the end of the beam. By subtracting the reversed run aver-

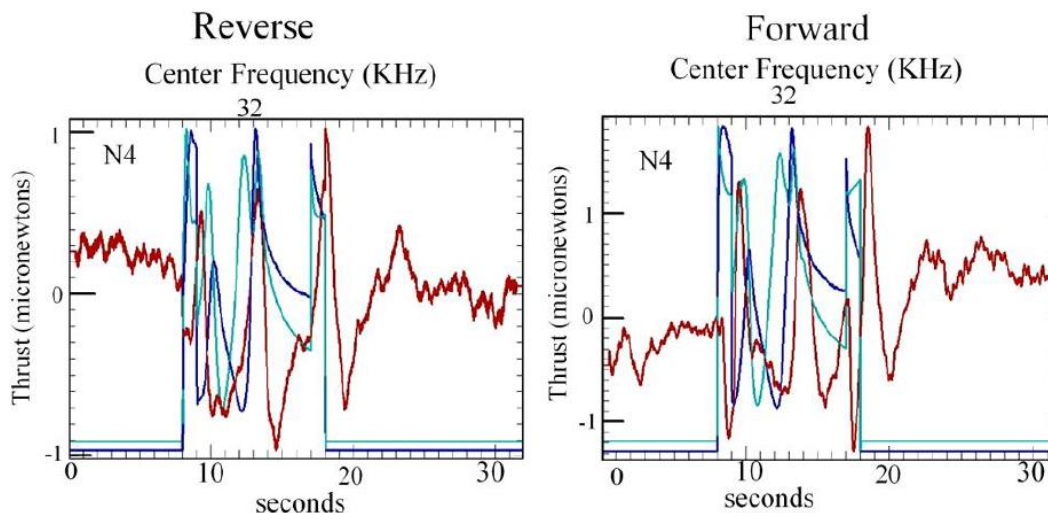


Figure 5(a) : Shows the forward and reverse runs. The red line shows thrust, note how it changes direction for the forward and reverse data. For both data sets, the red line first shows noise for 8 seconds before the first signal is applied. Then in the reverse data set the red line moves upward first then swings back with a damped motion, moves up again at the swept central frequency and finally the last 1 second pulse on resonance produces a large shift upward. In the forward data set, the red line shows noise for the first 8 seconds, then the acceleration goes downward and swings back. There is another downward spike at the swept central frequency, that is at 13 seconds, then the final 1 second resonant pulse gives another swing downward which then swings back and returns to noise. The light blue line is the accelerometer voltage and the dark blue line is the PZT stack voltage squared which is proportional to the power delivered to the PZT stack.

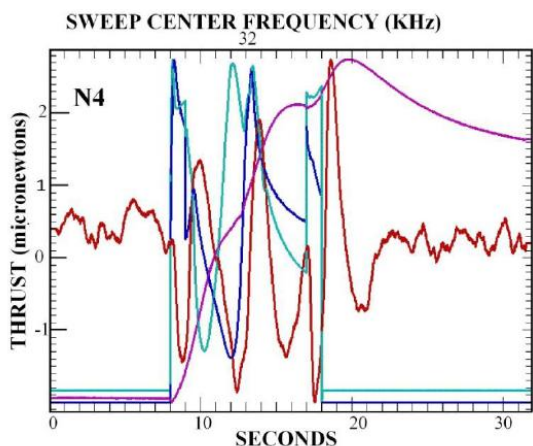


Figure 5(b) : This data set is the forward data minus the reverse data. The procedure will eliminate most of the noise. The figure shows a red line which is the thrust, a light blue line which is the accelerometer voltage and a dark blue line which is the PZT stack voltage squared, proportional to the power across the PZT stack. The blue lines are conveniently scaled to fit the graph. The thrust shown is approximately 1.5 μN . The center frequency was 32.35 KHz applied for 1 second, then a downward sweep of 10 KHz for 8 seconds and then a final resonant pulse for 1 second. The magenta line is the temperature measured by the thermistor embedded in the end cap. The temperature changes by only a few degrees centigrade per run.

age from the forward average, all signals that do not reverse with the direction of the device are eliminated by this procedure as they are “common mode”. This was easily the most important test applied. Other tests are described in ref.^[2].

Experimental results

Tests where a real thrust was sought employed a 1.27 cm brass reaction mass of 64.7 g. This configuration of the apparatus produced a thrust of approximately 1.5 μN . It is most clearly seen in Figure 5(b) where we have subtracted the reverse run from the forward run to eliminate common mode signals and noise. While one may reasonably expect the subtraction procedure to cancel signals produced by vibration in the apparatus (as the vibration must act on the bearings at the center of the thrust balance, a considerable distance from the device), the test reported in the next section was carried out to assure those interested that vibration was not the cause of the thrust signals seen.

NULL EXPERIMENT SETUP AND RESULTS

One of us [HF] recently attended a workshop, The Ad-

vanced Space Propulsion Workshop in Huntsville Alabama (ASPW 2012) and came back with an important suggestion for a null experiment^[10]. If we were to place identical brass masses on either side of our active PZT stack, then the mass fluctuations would result in pushes and pulls of equal magnitude and the device should just oscillate a little but show no average thrust. This was deemed to be worth testing. It would show that we were able to eliminate any unwanted vibration, noise effects. 0.635cm length brass masses were attached to either end of the PZT stack. A symmetric arrangement for the mount was used so as not to bias the forces in either direction. A central aluminum mounting ring with 3 screws arranged at 120 degree intervals which contacted plastic tabs glued onto the PZT stack performed this function. Care was taken not to short any of the electrodes which were embedded in between the PZT disks. See also the black heat shrink which was wrapped around each of the 4-40 threaded rods used to bind the device together, see Figure 6(b).

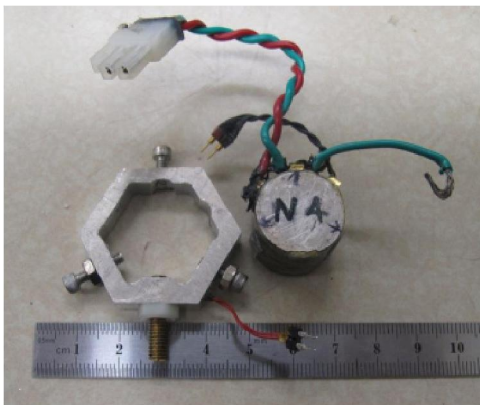


Figure 6(a) : The central mount bracket is made of aluminum. Note the red thermistor wire embedded in the aluminum. The PZT stack is also shown with a scale to approximate the size. The 3 tabs can be seen, on the left is the positive, center ground and right positive for the accelerometers.

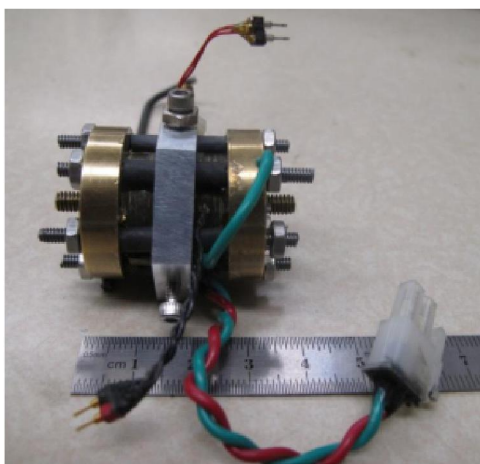


Figure 6(b) : The N4 stack now assembled with 1/4 inch long brass masses on each end. Note the twisted red/green power wires and the black accelerometer wire.

This device was then bolted into the Faraday cage, using the large brass screw shown in Figure 6(a), and mounted on the thrust balance shown in Figure 3. The experiment was run twice, once with a low power 70 volts and then with a higher applied voltage, 160 volts. There were difference resonant frequencies, 41.4 KHz (with voltage of about 70 V) and 42.4 KHz with a higher voltage of about 160V). The results for the resonant frequency 42.4kHz are shown in Figure 7. Both forward and reversed runs were acquired and averaged. Note that the thrust does not reverse direction in this case, as is shown in Figure 7c.

It is clear that if the higher power result shows a null in the thrust then so will the lower power result, which was indeed the case. Only the high power result is displayed. A center frequency pulse of 42.4 KHz was applied for 2 seconds, then a downward sweep of 10 KHz for 8 seconds, then a final center frequency pulse was applied for 2 seconds. As before the red lines in the graphs below shows the thrust. The light blue line is the accelerometer voltage and the dark blue line is the PZT stack voltage squared in convenient units to fit the scale.

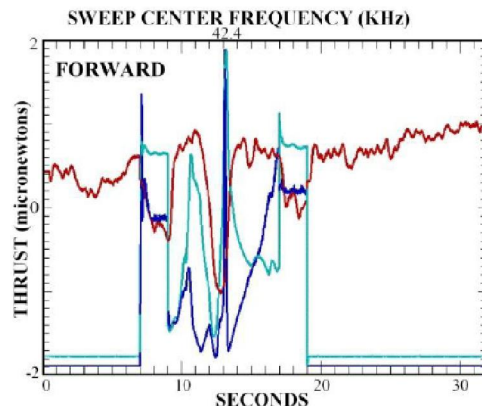


Figure 7(a) : Forward direction for 42.4KHz. The red line shows a central dip which occurs before the dark blue PZT stack voltage squared spike. Probably due to vibration. Resonant pulses applied for 2 seconds.

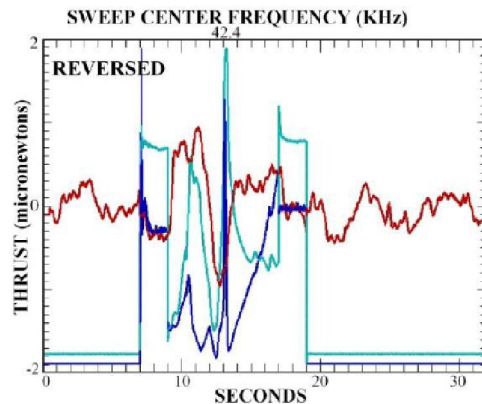


Figure 7(b) : The reversed run shows a dip roughly in the same spot and in the same direction as the forward run, evidently this is caused by vibration. Normal thrust signals would reverse direction.

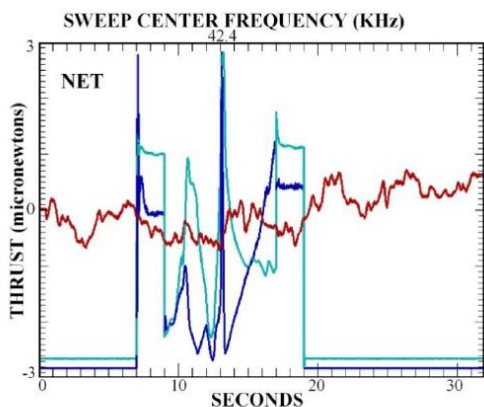


Figure 7(c) : This is the difference of the forward and reversed runs, or net effect, which shows no red line thrust, just noise. Any apparent oscillation can be thought of as due to resonant vibration of the device. There is clearly no thrust signal here. As before the light blue line represents the accelerometer voltage and the dark blue line is the PZT stack voltage squared, which is proportional to the power applied, divided by the impedance.

Clearly any thrust signal has been lost, and all that remains is noise, or a small oscillation on top of the noise due to the resonant frequency of the device. This is another test to show that vibration has been successfully damped out in the system, else a null result here for thrust would not have been possible.

CONCLUSIONS

A null experiment was performed to show that all vibrational effects have been eliminated from our data. When equal size reaction masses were attached to each end of the active PZT stack, the induced mass fluctuations push and pull in both directions at once. For this situation the device should not theoretically produce a net thrust. In Section 4 it was demonstrated that by using equal masses at both ends of our device the thrust can indeed be eliminated. This is a rather nice way to show that the protocols employed are sufficient to eliminate any systematic “Dean Drive” caused by vibration in the system.

In addition, it was determined that an optimal brass reaction mass is necessary to give maximal thrust. Several different brass reaction masses 64.7g, 80.9g, 96.8g, 112.6g and 128.3g were tried. We found that for this PZT stack, the preferred brass reaction mass 80.9g. The data is not displayed here since for a different device one would have to run this kind of test again. But it is clearly something that would be worthwhile to optimize the thrust for a given device. It is thought that using a new material like

PMN will allow us to run the device on resonance longer without any detrimental (depolarizing/aging) effects. Ways to cool the device are being explored.

ACKNOWLEDGEMENTS

We thank the referee for helpful comments and suggestions and a very detailed review. HF also thanks the physics department at California State University Fullerton for the opportunity to attend the Advanced Space Propulsion Workshop, in Huntsville Alabama 2012. HF acknowledges the interesting discussions at the workshop which were the motivation for the null experiment described in Section 4.

REFERENCES AND NOTES

- [1] H.Fearn, J.F.Woodward; Recent results of an investigation of Mach effects thrusters, 48th Joint propulsion conference, in Atlanta Georgia, 29th July – 1st August 2012, Published by the American Inst. of Aeronautics and Astronautics AIAA, (2012).
- [2] J.F.Woodward; Making starships and stargates, Springer The mechanical behavior of the system is treated on page 156, this shows longer resonant pulses. Dean drive effects are treated on page 164, Jan., (2013).
- [3] Vibrational modes of PZT-5A discs. See for example R1 mode, <http://web.ift.uib.no/~jankoc/thesis/> and Jan Kobach’s dissertation, <http://web.ift.uib.no/~jankoc/thesis/diss.pdf>
- [4] STEMINC Piezo webpage: http://www.steminc.com/piezo/PZ_property.asp
- [5] A.L.Kholkin, et al.; Journal. of Applied Phys., **89**(12), 8066-8073 (2001).
- [6] M.W.Hooker; Properties of PZT-based piezoelectric ceramics between -150 and 250 degree C, NASA/CR-1998-208708.
- [7] R.E.Newnham, et al.; Electrostriction: Nonlinear electromechanical coupling in solid dielectrics, J.Phys.Chem., **B101**, 10141-10150 (1997).
- [8] (a) S.I.Babic, C.Akyel; Magnetic force calculation between thin coaxial circular coils in air, IEEE Trans. on Magnetics, **44**(4), 445-452 (2008); (b) See also, Frederick Grover; Inductance calculations, Dover publications, NY, (1973).
- [9] C-Flex E-10 bearing data sheet, <http://www.c-flex.com/stiffnessproperties.html>
- [10] The issue of vibration in this apparatus has already been studied, see ref^[2] p164. This null test compliments the work described there